Journal of Zhejiang University SCIENCE A
ISSN 1009-3095 (Print); ISSN 1862-1775 (Online)
www.zju.edu.cn/jzus; www.springerlink.com
E-mail: jzus@zju.edu.cn

Adaptive sampling for mesh spectrum editing*

ZHAO Xiang-jun[1,2], ZHANG Hong-xin[†1], BAO Hu-jun[1]
([1]State Key Lab of CAD & CG, Zhejiang University, Hangzhou 310027, China)
([2]College of Computer Science and Engineering, Xuzhou Normal University, Xuzhou 221116, China)
[†]E-mail: zhx@cad.zju.edu.cn
Received Apr. 26, 2006; revision accepted May 16, 2006

Abstract: A mesh editing framework is presented in this paper, which integrates Free-Form Deformation (FFD) and geometry signal processing. By using simplified model from original mesh, the editing task can be accomplished with a few operations. We take the deformation of the proxy and the position coordinates of the mesh models as geometry signal. Wavelet analysis is employed to separate local detail information gracefully. The crucial innovation of this paper is a new adaptive regular sampling approach for our signal analysis based editing framework. In our approach, an original mesh is resampled and then refined iteratively which reflects optimization of our proposed spectrum preserving energy. As an extension of our spectrum editing scheme, the editing principle is applied to geometry details transferring, which brings satisfying results.

Key words: Mesh editing, Adaptive sampling, Digital geometry processing
doi:10.1631/jzus.2006.A1193 **Document code:** A **CLC number:** TP391

INTRODUCTION

Free-form surface editing plays an important part in geometric modeling, such as Free-Form Deformation (FFD), level of detail editing. Users need to be careful to avoid artifacts in the result surface. In this paper, we present a new mesh editing technique based on geometry signal wavelet analysis. It indirectly modifies vertex positions in spatial domain by the simple geometry proxy that is simplified from the original mesh, and performs filtering and enhancement in frequency domain.

This technique is able to produce desirable results with a few user interactions. Our key contribution is an intrinsic adaptive sampling approach of surface mesh with low spectrum distortion. Our mesh editing method needs to separate different scale details in virtue of geometry signal spectrum, which is distorted severely when the original surface is parameterized. Our approach can adaptively optimize the sampling mesh in a regular parameterization domain, in terms of the intrinsic relationship between the spectrum and the details.

There are four areas of mesh processing relevant to our work, including mesh deformation, mesh detail editing, geometry signal processing, and parameterization of triangle mesh. Mesh deformation usually can be classified as lattice-based FFD (Sederberg and Parry, 1986), curve-based (Singh and Fiume, 1998), and others. The FFD method controls deformations of the original mesh by the lattice geometry proxy. A representative curve-based method is Wires (Singh and Fiume, 1998) which directly attaches curves to mesh surface to achieve deformations. Essentially, the attached curves are also proxies. However, the former heavily depends on users' experience. In other words, users cannot control the influenced areas directly and design details elaborately. The later requires sketching the curve-proxy repeatedly, which may invoke more user interaction. Our method employs the simplified model as the editing proxy to avoid the aforementioned deficiencies.

* Project supported by the National Basic Research Program (973) of China (No. 2002CB312102), and the National Natural Science Foundation of China (Nos. 60021201, 60333010 and 60505001)

Mesh editing can be performed at various resolutions to achieve both global control and local editing (Forsey and Bartels, 1988; Zorin *et al.*, 1997; Kobbelt *et al.*, 1998). In particular, Kobbelt *et al.* introduced a multi-resolution editing technique of arbitrary topology mesh, in which the multi-resolution structure is established by using the mesh decimation algorithm and the detail encoding technique. Users perform editing operation at an appropriate coarse resolution. Original mesh details are superimposed upon the resulting mesh to achieve a final solution. This method only gives users limited interaction freedom. In contrast, the method in this paper can achieve better shape control by specifying the spectrum as distributed constraints over the editable mesh region. Moreover, it does not need a multi-resolution mesh representation which requires maintaining a fussy data structure.

By taking geometry attribute as digital signal, geometry signal processing can tackle the large geometry data much more conveniently (Guskov *et al.*, 1999; Gu *et al.*, 2002; Zhou, 2002). Especially, Zhou *et al.*(2002) introduced a unified framework of digital signal processing, by regularly sampling the spherical parameterization of an arbitrary mesh. Their method transforms the original geometry attribute into spherical signal and applies a large variety of the signal processing techniques. To avoid the spectrum distortion of parameterization, they proposed an adaptive sampling method which keeps the consistency between the sampling density and the vertex density of the original mesh, although the vertex density is not the intrinsic feature of mesh surface. While our sampling method fully considers the intrinsic feature of the geometry signal spectrum, and is able to preserve uninjured detail scale.

Mesh parameterization is the foundation of many mesh processing tasks. Usually the consistent parameterizations (Praun *et al.*, 2001; Kraevoy and Sheffer, 2004) usually first construct an aligned base model between two or among more models, and then perform parameterization of each patch on the base model. Single mesh parameterization was discussed in (Desbrun *et al.*, 2002). Yoshizawa *et al.*(2004) presented a fast and simple stretch-minimizing parameterization method, which starts from the Floater shape that preserves parameterization, and then optimizes the parameterization gradually by minimizing a weighted quadratic energy.

In order to deal with large-scale and complex mesh model, divide-and-conquer is a general strategy. Because of the simplicity and flexibility of triangle mesh, we mainly tackle triangle mesh which has the same topology as the planar disc.

The rest of the paper is organized as follows. In Section 2, we introduce the mesh editing principle based on the geometry signal wavelet analysis. In Section 3, we present a strategy to preserve consistency of parameterization, when the topological connectivity of the geometry proxy is modified. In Section 4, we provide several examples and extended applications of our method. Finally, we conclude and discuss future work.

MESH EDITING FRAMEWORK WITH GEOMETRY SIGNAL WAVELET ANALYSIS

Geometry signal is a generic term of all attributes adhering to mesh vertex, including position coordinates, normal vector, texture coordinates, reflection coefficients etc., which can be represented as a piecewise linear function (Zhou, 2002).

Spatial domain editing and frequency domain processing are two major aspects of our mesh editing method based on geometry signal wavelet analysis. For spatial domain editing, the simplified model is used as the geometry proxy. When the simplified model is modified, its deformations are converted into digital geometry signals which are filtered, enhanced or processed in frequency domain. Then the processed deformation signals are cumulated to the original model and the resulting model in 3D space is obtained. The main steps of our wavelet editing approach are:

1. Construct a parameterization P of mesh $\boldsymbol{M}$.

2. Simplify $\boldsymbol{M}$ to obtain a coarse mesh M_i by mesh decimation, and synchronously so does P to obtain P_i.

3. Modify M_i to obtain M_i', and fix the parameterization P_i.

4. Sample the geometric signal adaptively on the parameterized planar mesh.

5. Perform wavelet analysis to generate their frequency spectrum: $f_{\boldsymbol{M}}$, f_{M_i} and $f_{M_i'}$.

6. Combine the above three frequency spectra into one.

7. The resulting model M' is obtained from the inverse transformation and the inverse sampling.

If we transfer the deformation signal to the original mesh directly, the result is often unsatisfying. Hence, mesh editing with geometry signal analysis makes use of the reciprocal relation between the signals of the spatial domain and those of the frequency domain. The practical editing operations are processed in spatial domain, while signal filtering and enhancement are processed in frequency domain (Zhao *et al.*, 2004). There are three observations that should be noted:

First, the original model $\boldsymbol{M}$, the proxy model M_i and the modified version M_i' are processed separately. Therefore, the three interrelated models can be replaced by three arbitrary models, among which correspondence are maintained through consistent parameterizations. It can be extended to a general mesh processing framework, as illustrated in Fig.1 (see page 1198).

Second, in Step IV, we can design a frequency synthesizer $S(f_{\boldsymbol{M}}, f_{M_i}, f_{M_i'})$, with its wavelet inverse transform formula being represented as:

$$f_{\boldsymbol{M}'}(\boldsymbol{x}) = \int S(g_{\boldsymbol{M}}(\boldsymbol{\omega})\hat{f}_{\boldsymbol{M}}(\boldsymbol{\omega}), g_{M_i'}(\boldsymbol{\omega})\hat{f}_{M_i'}(\boldsymbol{\omega}), g_{M_i}(\boldsymbol{\omega})\hat{f}_{M_i}(\boldsymbol{\omega}))\hat{\psi}(\boldsymbol{\omega})\mathrm{d}\boldsymbol{\omega}, \quad (1)$$

where $\hat{\psi}(\boldsymbol{\omega})$ is a kernel function for wavelet inverse transform, and g denotes the filters of the three models.

Various filters and frequency synthesizer can be designed for different purposes. The filters commonly follow $g_{\boldsymbol{M}}(\boldsymbol{\omega}) = g_{M_i}(\boldsymbol{\omega})$, and the frequency synthesizer usually adopts the following: $f_{\boldsymbol{M}}' + g_{M_i}(f_{M_i'}' - f_{M_i}')$ (f' denotes the filtered spectrum signals). The filter g can be written in vector form, whose different components can use different filters.

Third, we use the 2D dyadic discrete wavelet. Spectrum analysis and synthesis are applied to each component of the vector signal.

ADAPTIVE SAMPLING WITH SPECTRUM PRESERVATION

Once 3D model is flattened over planar region, mesh and the geometry signals carried by it may be distorted. In this section, we present a novel approach on how to minimize the distortion.

Vertex density

Let $n(i)$ be the valence of vertex i, and $|\boldsymbol{M}|$ be the number of the vertices on $\boldsymbol{M}$. Let $A(\boldsymbol{M})$ and $A(\Delta)$ denote the total surface area of $\boldsymbol{M}$ and the area of the triangle Δ, respectively. Let $T(i)$ be the set of triangles, which is the 1-ring neighborhood domain of the vertex i. The vertex density on $\boldsymbol{M}$ is given by

$$d_{\boldsymbol{M}}(\boldsymbol{x}) = \begin{cases} (n(i)+1)/(|\boldsymbol{M}| \sum_{\Delta \in T(i)} A(\Delta)/A(\boldsymbol{M})), & \boldsymbol{x} \in V_{\boldsymbol{M}}, \\ \alpha d_{\boldsymbol{M}}(x_i) + \beta d_{\boldsymbol{M}}(x_j) + \gamma d_{\boldsymbol{M}}(x_k), & \boldsymbol{x} \in (i,j,k), \end{cases} \quad (2)$$

where $V_{\boldsymbol{M}}$ is the vertex set of $\boldsymbol{M}$, (i,j,k) is a triangle on $\boldsymbol{M}$, and (α,β,γ) are the barycentric coordinates of $\boldsymbol{x}$

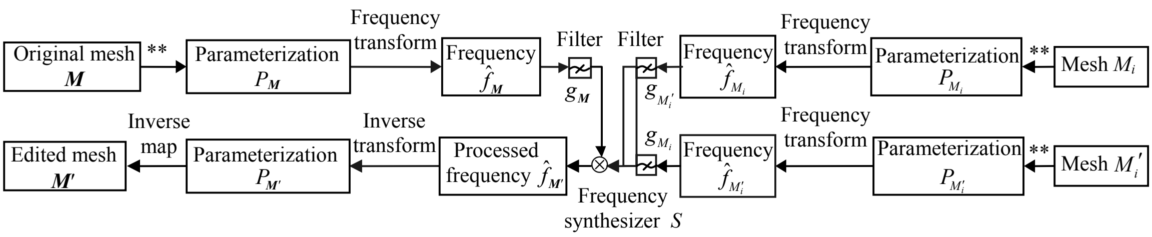

Fig.1 Mesh editing diagram based on geometry signal wavelet analysis
** denotes that their consistent parameterizations are performed

with respect to (i,j,k). Note that the vertex density is normalized to ensure that it is independent on scale.

Parameterization and geometry signal spectrum

Zhou (2002) discussed the difference of spectral signal carried on the planar curves when the topology homogeny transformation is performed. He concluded that the vertex density distribution of the sampling mesh should be consistent with that of the original mesh.

As illustrated in Fig.2, a set of shape points spans a continuous curve. Accordingly, the distribution of the shape points should not affect the sampling of the original curve. The discrete sampling of the continuous curve can include the following cases:

(1) Sampling sparsely where the curvature is less, and densely where the curvature is large, e.g., the curve segment *AB* in Fig.2.

(2) Sampling along the curve uniformly, e.g., the curve segment *CD* in Fig.2.

(3) Contrary to Case (1), sampling sparsely where the curvature is large and densely where the curvature is less, e.g., the curve segment *BC* in Fig.2.

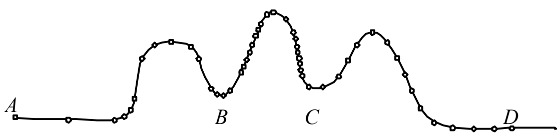

Fig.2 Three sampling cases (*AB*, *BC*, *CD*) of a continuous curve

We can see that the adaptive sampling should not depend on the vertex density distribution. The right way is to sample the given curve uniformly along the parameter axes, which keeps the spectrum of the new signal the same as that of the original curve, just like the sampling method of curve segment *CD*.

The key observation in curve cases can be applied to the spatial surface. Let M_R be a resampled 3D model. If the vertices of M_R are distributed uniformly, the sampling signals can preserve well the original feature. There exists a bijection $\Pi_{M\text{-}R}$ between the original mesh M and the sampling one R. The vertices on R are adjusted iteratively and symmultaneously those on M_R are updated until the following inequality is satisfied (Zhou, 2002):

$$|R|^{-1}\sum\left|D_M(\Pi^{-1}_{M\text{-}R}(\{i\}))-\overline{D}_{M_R}\right|<\varepsilon,\ i\in R, \quad (3)$$

where $\overline{D}_{M_R}=\sum_{i\in R}D_M(\Pi^{-1}_{M\text{-}R}(\{i\}))/|R|$ is the average vertex density of M_R, $|\cdot|$ denotes the number of mesh vertices, and ε is a predefined threshold.

Adaptive sampling strategy

Highly uniform resampled mesh brings low spectrum distortion. Usually, the following energy function can be used to guide the optimization of the adaptive sampling mesh.

$$E(V)=\frac{1}{2}\sum_i\sum_{j\in N_i}w(\boldsymbol{v}_j)\,\|\boldsymbol{v}_i-\boldsymbol{v}_j\|^2, \quad (4)$$

where N_i is the set of 1-ring neighborhood of the vertex $\{i\}$, $\boldsymbol{v}_i\in V_{M_R}$, V is the set composed of $\boldsymbol{v}_i$, and $\|\cdot\|$ is the L^2-norm. $w(\boldsymbol{v}_j)$ is the weight function (shape function). Precisely, the weight function is

$$w(\boldsymbol{v}_j)=\frac{\overline{D}_{M_R}+p}{D_{M_R}(j)+p},\ p\in\mathbb{R}^+, \quad (5)$$

where $D_{M_R}(j)$ is the vertex density at vertex $\{j\}$ in M_R, and $\overline{D}_{M_R}$ is the average vertex density of M_R. When $D_{M_R}(j)$ is less than $\overline{D}_{M_R}$, $w(\boldsymbol{v}_j)$ is greater than 1, and the vertex $\{i\}$ comes near to $\{j\}$.

By our consistent parameterization, a corresponding planar point can be found timely for each vertex in the original 3D mesh. Since the point on the parametric plane can be adjusted effectively, an optimization is carried out on the parametric domain.

First, we assume that $\boldsymbol{u}_i\in V_R$, which corresponds to $\boldsymbol{v}_i$. $\boldsymbol{v}_i$ is located in the triangle $T=\Delta\boldsymbol{q}_1\boldsymbol{q}_2\boldsymbol{q}_3$ of the original model, $\boldsymbol{u}_i$ is located in the triangle $T'=\Delta\boldsymbol{p}_1\boldsymbol{p}_2\boldsymbol{p}_3$ of the parameterization mesh, and T' corresponds to T. The barycentric coordinates of $\boldsymbol{u}_i$ are $(\alpha_i,\beta_i,1-\alpha_i-\beta_i)$, where $\alpha_i<\boldsymbol{u}_i,\boldsymbol{p}_2,\boldsymbol{p}_3>/A$, $\beta_i<\boldsymbol{u}_i,\boldsymbol{p}_3,\boldsymbol{p}_1>/A$, and A is the area of T'. So it is known that there is an affine mapping between $\boldsymbol{u}_i$ and $\boldsymbol{v}_i$. $S:\mathbb{R}^2\rightarrow\mathbb{R}^3$, and $\boldsymbol{v}_i=S(\boldsymbol{u}_i)=\alpha_i\boldsymbol{q}_1+\beta_i\boldsymbol{q}_2+(1-\alpha_i-\beta_i)\boldsymbol{q}_3$.

In order to make vertices on the resampled mesh as uniform as possible, the energy function $E(\boldsymbol{V})$

should be minimized. It means that $\partial E/\partial \boldsymbol{u}_i=0$ should be satisfied. Therefore, we have:

$$\sum_{j\in N_i}\left\{(w(S(\boldsymbol{u}_j))+w(S(\boldsymbol{u}_i)))\left(\left(\frac{\partial S}{\partial \boldsymbol{u}_i}\right)^{\mathrm{T}}(S(\boldsymbol{u}_i)-S(\boldsymbol{u}_j))\right)\right.$$
$$\left.+\frac{1}{2}\left(\left(\frac{\partial S}{\partial \boldsymbol{u}_i}\right)^{\mathrm{T}}\frac{\partial w}{\partial S}\right)\|S(\boldsymbol{u}_j)-S(\boldsymbol{u}_i)\|^2\right\}=0. \tag{6}$$

From Eqs.(2) and (5), when the sampling mesh is dense enough, the polygon constructed by the 1-ring neighborhood of $\{i\}$ is planar approximately, and the shape function $w(\boldsymbol{v}_i)$ does not vary sharply with the movement of $\boldsymbol{v}_i$ in the polygon. That is $\partial w/\partial S=(0,0,0)^{\mathrm{T}}$. Let $\boldsymbol{u}=(s,t)^{\mathrm{T}}$, we have:

$$\begin{cases}\partial S/\partial s=(\boldsymbol{q}_1(p_{2,2}-p_{3,2})+\boldsymbol{q}_2(p_{3,2}-p_{1,2})\\ \qquad +\boldsymbol{q}_3(p_{1,2}-p_{2,2}))/(2A),\\ \partial S/\partial t=(\boldsymbol{q}_1(p_{3,1}-p_{2,1})+\boldsymbol{q}_2(p_{1,1}-p_{3,1})\\ \qquad +\boldsymbol{q}_3(p_{2,1}-p_{1,1}))/(2A).\end{cases} \tag{7}$$

Denote $\partial S/\partial \boldsymbol{u}_i=\boldsymbol{M}$, where S is a 3-vector, and $\boldsymbol{M}$ is a 3×2 matrix. Let

$$\boldsymbol{B}=2A\frac{\sum_{j\in N_i}\{(w(\boldsymbol{v}_j)+w(\boldsymbol{v}_i))(\boldsymbol{M}^{\mathrm{T}}\boldsymbol{v}_j)\}}{\sum_{j\in N_i}(w(\boldsymbol{v}_j)+w(\boldsymbol{v}_i))},$$

then Eq.(6) can be transformed into:

$$\langle\boldsymbol{u},\boldsymbol{p}_2,\boldsymbol{p}_3\rangle(\boldsymbol{M}^{\mathrm{T}}(\boldsymbol{q}_1-\boldsymbol{q}_3))+\langle\boldsymbol{u},\boldsymbol{p}_3,\boldsymbol{p}_1\rangle(\boldsymbol{M}^{\mathrm{T}}(\boldsymbol{q}_2-\boldsymbol{q}_3))$$
$$=\boldsymbol{B}-\langle\boldsymbol{p}_1,\boldsymbol{p}_2,\boldsymbol{p}_3\rangle(\boldsymbol{M}^{\mathrm{T}}\boldsymbol{q}_3). \tag{8}$$

Denote $\boldsymbol{C}=\begin{pmatrix}\boldsymbol{M}^{\mathrm{T}}(\boldsymbol{q}_1-\boldsymbol{q}_3)\\ \boldsymbol{M}^{\mathrm{T}}(\boldsymbol{q}_2-\boldsymbol{q}_3)\end{pmatrix}$, and $\boldsymbol{B}'=\boldsymbol{B}-\langle p_1,p_2,p_3\rangle\times(\boldsymbol{M}^{\mathrm{T}}\boldsymbol{q}_3)$. The solution of Eq.(8) is as follows

$$\boldsymbol{u}=\frac{1}{Deno}(D_1\boldsymbol{p}_1+D_2\boldsymbol{p}_2+D_3\boldsymbol{p}_3)\odot\boldsymbol{B}_1'+\boldsymbol{p}_3, \tag{9}$$

where

$$\boldsymbol{D}=(C_{22}-C_{12},-(C_{21}-C_{11}),(C_{21}-C_{11})-(C_{22}-C_{12})),$$

$$Deno=-\begin{vmatrix}1&1&1\\p_{11}&p_{21}&p_{31}\\p_{12}&p_{22}&p_{32}\end{vmatrix}|\boldsymbol{C}|,$$

and $\odot$ denotes the element-by-element product of the two vectors.

The new weights should be updated in each iteration until $\|\boldsymbol{u}^{l+1}-\boldsymbol{u}^{l}\|<\varepsilon$, where ε is a user-specified threshold. In general, when a 1-ring neighborhood polygon on sampling mesh spans several triangles of the parameterization mesh, the affine transformation S should be updated instantly in every iteration. After the iteration is fulfilled, the resulted sampling mesh in plane is what we need.

IMPLEMENTATIONS AND ALGORITHM EXTENSIONS

All the algorithms in the paper have been implemented using VC++ 7.0. A modified Half-Edge data structure without inner loop is adopted to represent triangle mesh. All the examples are produced by our prototype system. In general, some preprocessing tasks, such as global parameterization and generation of the adaptive sampling mesh, are performed first, and our editing algorithm can achieve the response speed in real time.

Adaptive sampling

We have achieved the adaptive sampling method. Fig.3 (see page 1198) shows the compared results of the three methods, our adaptive sampling, the evenly regular sampling method and the sampling by (Zhou, 2002). Fig.3a is the original model. Figs.3b~3e are the results of our method, Figs.3f~3i are the results of the regular method and Figs.3m~3p are the results of (Zhou, 2002).

The local compared results of our method and (Zhou, 2002) are illustrated in Fig.4 (see page 1199).

Mesh deformation

By using Daubechies 3 wavelet base functions and setting different filters, a set of editing results is produced, shown as Figs.5a~5e. The wavelet transform constructed from compactly supported wavelet basis, is local transformation on the time-frequency

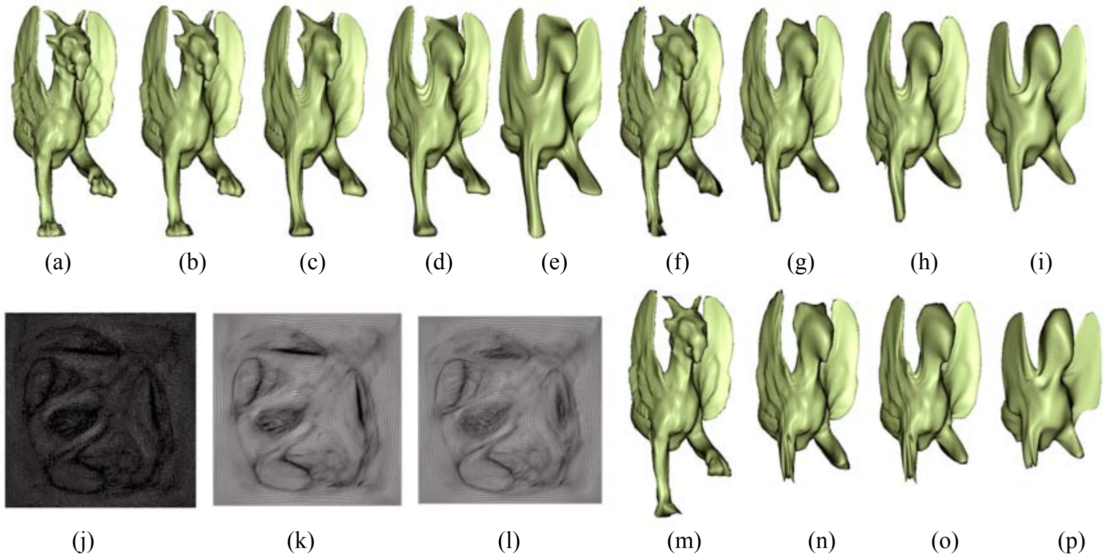

Fig.3 The compared results of the three methods: our adaptive sampling, the regular sampling and the sampling by (Zhou, 2002). (a) is the original model; (b) is the model of our method, and (c)~(e) are the three different filtering results of our method; (f) is a regular resample mesh, and (g)~(i) are the three different filtering results; (m) is the model of (Zhou, 2002), and (n)~(p) are the three different filtering results; (j) is the parameterization of (a); (k) and (l) are the resample meshes of the (b) and (m), respectively; (c), (g), (n) are used by the same filtering method, and so do (d), (h), (o) and (e), (i), (p)

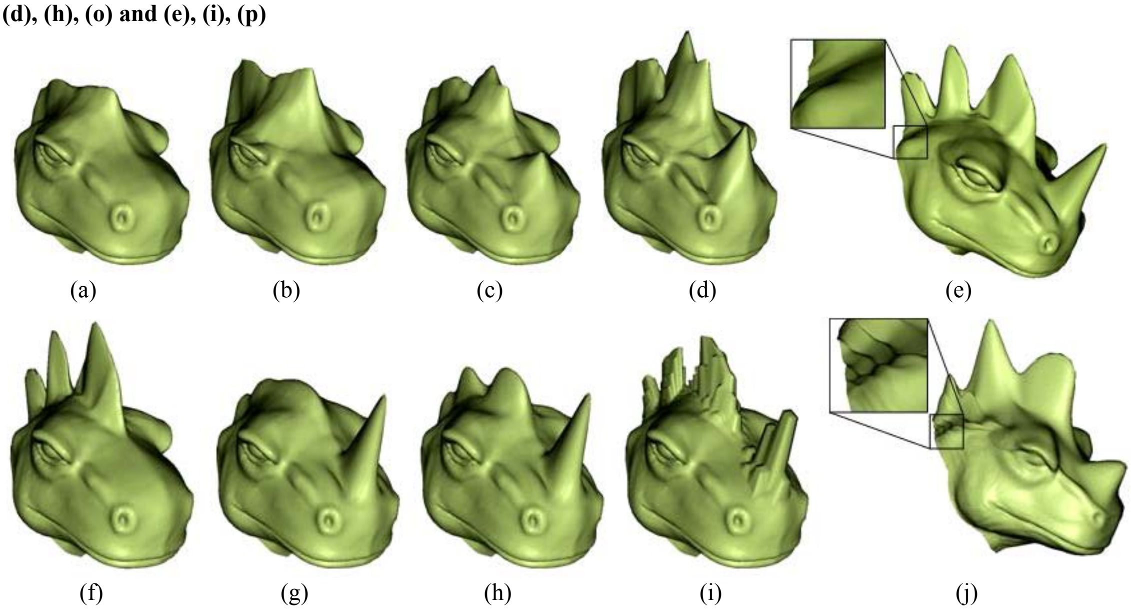

Fig.5 Wavelet editing results of the crocodile head model. (a)~(e) Wavelet editing results with different filters; (f)~(h) Editing results with different filters on the head horn and the face horn; (i) The editing result based on Haar wavelet; (j) The Fourier editing result. The zoom-in region shows some unexpected wrinkles and drapes

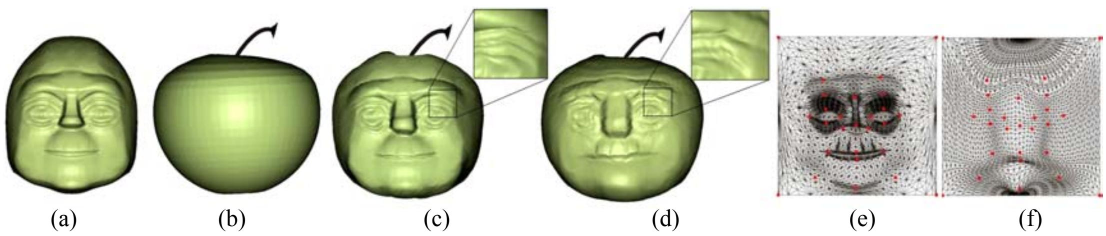

Fig.6 Detail transferring. (a) YODA model; (b) Apple model; (c), (d) The editing results of wavelet-based method and Fourier-based method, respectively; (e), (f) Consistent parameterizations of YODA and Apple

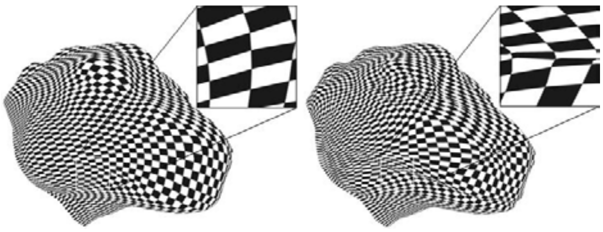

(a) (b)

Fig.4 The adaptive sampling mesh is obtained by (a) our method and (b) the one by Zhou (2002).

domain. Therefore, local high and low frequency components can be decomposed efficiently from geometry signals by multi-scale resolution analysis. Compared with the Fourier spectrum editing approach, the wavelet editing separates the local and global information better. And after such processing as filtering and enhancement, the wavelet editing can obtain more desirable results. The offset in frequency domain of the wavelet space corresponds to its space position. Hence it is convenient to process sub-regions respectively. The Fourier spectrum editing approach readily produces blurred detail, unexpected wrinkles and drapes, as shown in Fig.5j (see page 1198). Yet the wavelet editing can avoid those problems. The wavelet editing framework allows us to adopt different wavelets in different regions. The flexibility can enrich editing results, as illustrated in Figs.5f~5h. Using Haar wavelet to filter, we get a special editing effect shown in Fig.5i.

Detail transferring

The local detail of the 3D model corresponds to the high frequency component. Therefore, the high frequency component can be used as deformation signal and can be cumulated to the object model by the wavelet editing approach. Exactly speaking, in order to transfer the detail of M_a to M_b, we assume that $M_{a'}$ is the high frequency component of M_a that is filtered to. By replacing the signal suffixes of the wavelet editing formula as follows: $M_b \leftarrow \boldsymbol{M}$, $M_a \leftarrow M_i'$, $M_{a'} \leftarrow M_i$, we use indiscriminately the wavelet editing flow. Fig.6 shows the result that YODA's face details are transferred to the Apple model. For comparison, we also show the result of the Fourier editing. It turns out that the wavelet editing is superior to the Fourier editing, and the resulted detail of the former is finer than that of the later.

CONCLUSION AND FUTURE WORK

To fight against the shortcomings of traditional method of triangle mesh editing, we propose a unified framework of mesh editing method with the geometry signal wavelet transformation. In order to sketch the edited region correctly, we introduce a strategy of mesh editing method by the consistent parameterization. According to the relationship between sampling and frequency preservation of geometry signal, we put forward a new adaptive sampling method. Our method combines the advantages of spatial domain with the one of frequency domain, which can directly manipulate the simplified mesh. Moreover, the manipulation is easy and uniform. The inherent procedure pattern of deformation transferring and filtering is efficient and concise. Experiments showed that our editing method prefers to extract geometry detail and tailors the filter in different regions.

Our future work is to amend such key technologies as consistent parameterization and adaptive sampling. It is aimed at attempting to find other analysis tools and to exploit such research as the accelerated algorithm of programmable hardware GPU.

References

Desbrun, M., Meyer, M., Alliez, P., 2002. Intrinsic parameterizations of surface meshes. *Computer Graphics Forum*, **21**(3):209-218. [doi:10.1111/1467-8659.00580]

Forsey, D.R., Bartels, R.H., 1988. Hierarchical B-spline refinement. *Computer Graphics Proceedings, (SIGGRAPH'88)*, **22**(4):205-212. [doi:10.1145/378456.378512]

Gu, X.F., Gortler, S., Hoppe, H., 2002. Geometry images. *ACM Trans. Graph (SIGGRAPH'02)*, **21**(3):355-361.

Guskov, I., Sweldens, W., Schröder, P., 1999. Multiresolution signal processing for meshes. *Computer Graphics (SIGGRAPH'99)*, **33**:325-334.

Kobbelt, L., Campagna, S., Vorsatz, J., Seidel, H.P., 1998. Interactive multiresolution modeling on arbitrary meshes. *Computer Graphics (SIGGRAPH'98)*, **32**:105-144.

Kraevoy, V., Sheffer, A., 2004. Cross-parameterization and compatible remeshing of 3D models. *ACM Trans. Graph.*, **23**(3):861-869. [doi:10.1145/1015706.1015811]

Praun, E., Sweldens, W., Schröder, P., 2001. Consistent mesh parameterization. ACM Proc. SIGGRAPH'01, p.179-184.
Sederberg, T.W., Parry, S.R., 1986. Free-form deformation of solid geometric models. *Computer Graphics (SIGGRAPH'86)*, **20**(4):151-160. [doi:10.1145/15886.15903]
Singh, K., Fiume, E., 1998. Wires: A geometric deformation technique. *Computer Graphics (SIGGRAPH'98)*, **32**:405-414.
Yoshizawa, S., Belyaev, A., Seidel, H.P., 2004. A Fast and Simple Stretch-Minimizing Mesh Parameterization. Proceedings of the Shape Modelling International 2004 (SMI'04), IEEE Computer Society.
Zhao, X.J., Zhang, H.X., Bao, H.J., 2004. Mesh editing based on geometry signal spectrum analysis. *Journal of Software*, **15**(suppl.):149-156 (in Chinese).
Zhou, K., 2002. Digital Geometry Processing: Theory and Applications. Ph.D Thesis, Zhejiang University, Hangzhou, China (in Chinese).
Zorin, D., Schröder, P., Sweldens, W., 1997. Interactive multiresolution mesh editing. *Computer Graphics (SIGGRAPH'97)*, **31**:259-268.